Organic Electronics 15 (2014) 3746–3755

Contents lists available at ScienceDirect

Organic Electronics

journal homepage: www.elsevier.com/locate/orgel

Experimental comparison of high-performance water vapor permeation measurement methods

Giovanni Nisato [a,*], Hannes Klumbies [b], John Fahlteich [c], Lars Müller-Meskamp [b], Peter van de Weijer [d], Piet Bouten [d], Christine Boeffel [e], David Leunberger [a], Wülf Graehlert [f], Steven Edge [g], Stéphane Cros [h], Paul Brewer [i], Esra Kucukpinar [j], Julia de Girolamo [k], Padmanabhan Srinivasan [l]

[a] CSEM Centre Suisse d'Électronique et de Microtechnique SA, Muttenz, Switzerland
[b] Institut für Angewandte Photophysik IAPP at Technical University of Dresden, Dresden, Germany
[c] Fraunhofer Institute for Electron Beam and Plasma Technology FEP, Dresden, Germany
[d] Philips Research Laboratories, Eindhoven, The Netherlands and Holst Centre, High Tech Campus, Eindhoven, The Netherlands
[e] Fraunhofer Institute for Applied Polymer Research IAP, Potsdam-Golm, Germany
[f] Fraunhofer Institute for Material and Beam Technology IWS, Dresden, Germany
[g] The Centre for Process Innovation (CPI), NETPark, Sedgefield, Co Durham, TS21 3FG, United Kingdom
[h] Institut National De L'Energie Solaire CEA-INES, Le Bourget-du-Lac, France
[i] National Physical Laboratory, Hampton Road, Middlesex TW11 0LW, United Kingdom
[j] Fraunhofer Institute for Process Engineering and Packaging IVV, Freising, Germany
[k] CEA-LITEN, Grenoble, France
[l] Solvay Specialty Polymers, Bollate, Italy

ARTICLE INFO

Article history:
Received 30 July 2014
Received in revised form 7 October 2014
Accepted 12 October 2014
Available online 28 October 2014

Keywords:
WVTR
Calcium test
TDLAS
CRDS
IMMS
Coulometric test

ABSTRACT

The requirement for evaluating high performance barrier layers with water vapor transmission rates (WVTR) far below 10^{-3} g/m^2 d has been sparked by the growing application of flexible and organic electronics. While several highly sensitive WVTR-measurement techniques are described in the literature, their accuracy and comparability has not yet been tested. There is an absence of direct comparison of these methods. With a growing body of literature referring to different coating and barrier technologies (often under different testing conditions), it is extremely difficult to gather a coherent picture both of the performance of the materials studied and the permeation measurement methods used. In order to clarify these points we report on independent WVTR measurements of the same batch of a high performance barrier film under two sets of conditions in several laboratories with different state-of the-art methods. These methods also include several calcium test set-ups. The results showed that, while some differences are present, there is a remarkable level of agreement between the measurement methods even prior to harmonization.

1. Introduction

Printable and organic large area electronic devices are in production and continue to be the subject of further research and development, with the perspective to profoundly impact application areas such as displays, general lighting and photovoltaic energy production. Due to the sensitivity of the device stacks to oxygen and water it was recognized very early that a realistic application of these technologies would have to rely on effective high performance permeation barrier materials, to protect the

* Corresponding author.

http://dx.doi.org/10.1016/j.orgel.2014.10.014
1566-1199/

devices and reduce the effect of external conditions on the devices' lifetime. In this context, the determination of the ingress of water vapor as well as oxygen from a qualitative and quantitative point of view is of primary interest.

Often the organic devices themselves offer the best and most sensitive indicators of performance of permeation barrier materials, however they can be time-consuming and expensive to fabricate, they are not standardized, and not all barrier materials researchers have this capability.

The development of barrier materials requires very sensitive permeation detection methods with low detection limits, reasonably short measurement times and the possibility to detect different defects and permeation moieties. A clear hurdle is the low detection limit required by many applications, which is below the threshold of commonly used commercially available equipment. This leads to the development of alternative measurement methods including one of the most widely used family of methods: the "calcium test" [1]. A large number of research groups use different variations of these methods to characterize different high performance barrier systems under different experimental conditions (temperature, relative humidity) depending on their application requirements or simply due to equipment limitations. This leads to the questions of whether the barrier properties measured are condition-dependent and whether there are ways to compare them across different laboratories. There is a common need to identify acceleration factors to relate permeation rates at different temperature and relative humidity to help translate from one condition to another. Further, it has to be identified and clarified whether the best possible (intrinsic) performance of a barrier or material is measured or whether a more technologically realistic and relevant system (effective performance including defects but not edge leakage) is being investigated. Finally, the aim of many studies is to present the performance of specific barrier systems, not to evaluate the measurement technique used to characterize them; very few groups are able to perform measurements using more than one technique. Together, these points lead to a large variety of publicly communicated results that are not in clear agreement, ultimately creating a certain amount of confusion both concerning the characterization methods and the performance of the thin-film barrier materials being developed.

The purpose of this paper is to present the first pragmatic and systematic comparison of high performance water vapor permeation methods for thin film barrier coatings. We do not address oxygen permeation, though several of the presented methods can be adapted to measure oxygen permeation as well.

The experimental approach we followed was to reduce as much as possible sources of inter-laboratory variations which are linked to barrier system variation, sample preparation and variation of operation conditions (temperature and relative humidity) of the tests, while leaving the experimental freedom of the laboratories to perform the tests using their usual analysis methods. We compared the same nominal materials in the same nominal conditions using extremely different permeation test methods, ranging from optical and electrical implementations of the calcium test measurement to commercially available water vapor permeation testing setups (in two laboratories) and to Cavity Ring-Down Spectroscopy (CRDS) as well as Tunable Diode Laser Absorption Spectroscopy (TDLAS) and Isotope Marking Mass Spectrometry (IMMS).

2. Background regarding Water transmission measurements

Handling, pre-conditioning as well as the terminology are general points we would like to clarify here. For the ease of clarity in the usage of terms, we emphasize to solely use "WVTR" (water vapor transmission rate) for effective, steady-state permeation through a barrier film. Other meanings could be expressed with "transient" (for the initial WVTR before reaching a steady state) and "intrinsic" (barrier without defects).

Concerning the intrinsic WVTR, it should be noted that though it is measured on defect free parts of the sample it does not necessarily relate only to Fickian diffusion through the layer material. Small defects like grain boundaries in polycrystalline materials contribute non-Fickian diffusion to the intrinsic WVTR value [2]. All methods described in this paper can measure the effective WVTR, but only the optical calcium test monitored with a CCD-camera is capable of measuring the intrinsic WVTR in one measurement with the effective WVTR. The intrinsic WVTR may be lower than the effective WVTR by orders of magnitude and should be explicitly named to avoid confusion. The ratio between intrinsic and effective permeation gives an indirect measurement of the (point) defects present in a given barrier system. Intrinsic permeation is the lower possible bound for a given encapsulation technology. Intrinsic properties are very important from the perspective of fundamental understanding and materials science, and can be obtained on samples with small surface areas (mm^2 or sometimes less), while effective properties are of technological and commercial relevance as the devices produced typically have hundreds of cm^2 of surface area at least. Reports in the literature rarely distinguish these two aspects. The different types (intrinsic and effective) have merit depending on the specific device technologies to which an encapsulation technique is applied to and their related degradation sensitivities. For instance, display applications critically dependent on each and every pixel quality, an intrinsic permeation value may be at the very least misleading since it makes no sense to measure a barrier that is locally excellent but has spatial variations of quality (point defects) that would preclude it anyway from being applied. For device applications less sensitive to point defects, an effective permeation value is the more appropriate quantity to be measured. For example, an organic photovoltaic module overall efficiency may decrease due to point defect diffusion leading to local degradation, but it may still be sufficiently functional for a given application. Therefore, it is advisable to indicate whether the technique or the data analysis methods deployed is yielding intrinsic or effective permeation values. Note that for a multilayer barrier even the optical calcium test can only exclude defects in the last barrier layer that is the barrier layer adjacent to the calcium. Hence, in a

multilayer high performance barrier system, the measurable intrinsic WVTR is the intrinsic WVTR of the last barrier layer plus an indirect measurement of the effective WVTR of the underlying part of the barrier stack.

Depending on the history of the sample, organic interlayers sandwiched between the barrier layers may be anywhere between free or full of water, which strongly influences the transient WVTR [3]. To establish the final water gradient, i.e. to overcome the transient, those internal reservoirs have to be filled or emptied via the barrier layers. Consequently, the transient WVTR can be both, lower and higher than the steady-state WVTR. Often, multi-layer barrier layers slow down this establishment of the water gradient. Hence, the minimum transient duration set by the barrier film itself depends on the preconditioning of the sample and can exceed any practical measurement time or even a specified device lifetime [4]. In some cases, this distinction between the transient and steady-state regime may be of purely academic interest as researchers and technologists may be looking for a pragmatic means to measure water ingress to estimate a device lifetime, not to determine a scientifically accurate measurement. Furthermore, many measurement setups require a gas volume behind the barrier and, therefore, possess surfaces that can take up or outgas water: since a monolayer of water consists of roughly 3×10^{-4} g/m^2, i.e. an amount of water that requires months to permeate through an ultra-high barrier (WVTR 10^{-5}–10^{-6} g/(m^2 d) of the same area, water-adsorption at and -desorption from inner walls can strongly elongate the transient duration. Fig. 1 illustrates transient permeation through ideally dry barrier samples from the beginning of the measurement until reaching steady state. Fig. 1 is based on model calculations according to Fick's second law using Eq. (1) [4]:

$$Q(t) = \frac{DtC_1}{d} - \frac{dC_1}{6} - \frac{2dC_1}{\pi^2}\sum_{n=1}^{\infty}\frac{(-1)^n}{n^2}e^{-Dn^2\pi^2 t/d^2} \quad (1)$$

In this equation, D is the diffusion coefficient of the barrier film, C_1 describes the moisture concentration on the wet side of the measurement cell, d is the thickness of the film, t is the time and $Q(t)$ describes the total amount of permeated water. Note that Fickian diffusion strictly speaking applies to a homogeneous material having a constant diffusion coefficient. In multilayer barriers, gas transport occurs through defects and has to overcome distances in the polymer interlayer to reach defects in the subsequent barrier layer. While a multilayer barrier is no homogeneous material, the gas transport through polymer layers (as main driver for increased lag-time) can be approximated as Fickian diffusion. Hence, a multi-layer system can also exhibit delayed gas diffusion (lag times) as described in Fick's second law. Hence for the case shown in Fig. 1, stopping the measurement too early would lead to the assumption that the multilayer barrier shows a much better barrier performance although the steady state WVTR is much higher than for the single layer. This again underlines the importance of not stopping the measurement too early if steady-state permeation is the quantity one wants to acquire.

However, for durations exceeding the device lifetime, the transient and not the steady-state permeation is of interest, anyway. This is especially true under real conditions, e.g. in the presence of sunlight for solar cells, where the barrier itself may be subjected to aging, i.e. steady-state permeation changes with time. For integration methods like the calcium test, some amount of water needs to be accumulated to observe a change: a WVTR of 1×10^{-4} g/(m^2 d) consumes 1 nm of calcium within

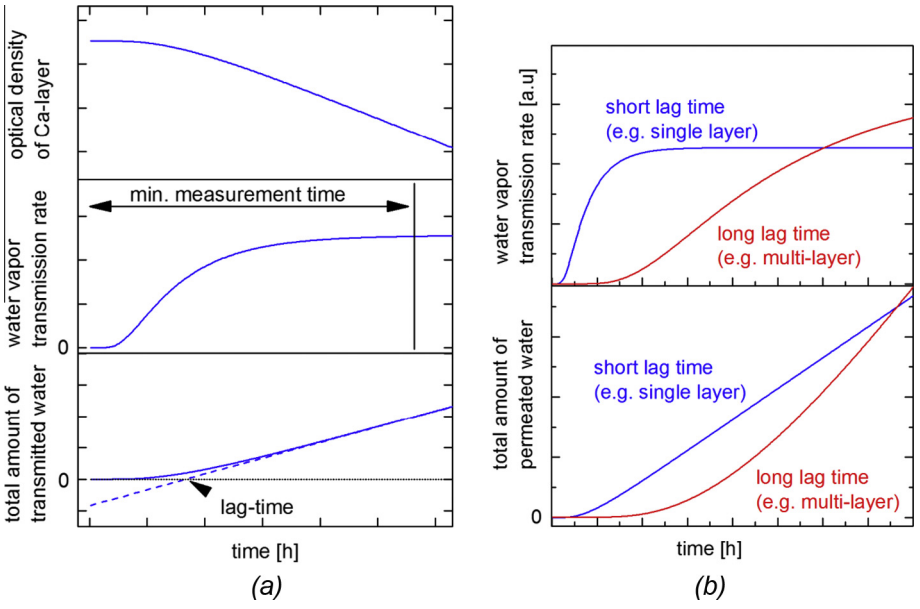

Fig. 1. Schematic representation of the time-dependent permeation through initially dry barrier films calculated from Fick's second law according to the equations given in [4]: (a) comparison of lag time, measurement time and increase of optical transmittance of calcium over time and (b) illustration of potential misinterpretation of multilayer barriers having a long lag-time but a poor steady-state WVTR.

14 days, a WVTR of 1×10^{-5} g/(m^2 d) requires 140 days. Taking all discussed effects into account, we want to stress, that measuring the WVTR of an ultra-high barrier can be very time-consuming, e.g. several months. A solution is to evaluate the WVTR at elevated temperatures and humidity and then extrapolate the WVTR to operating conditions. Thereby, the acceleration factor between both conditions has to be known. First, there can be an acceleration due to more water vapor in the air. For example, 100% r.h. at 20 °C equal 23 hPa (Magnus formula [5]) while 100% r.h. at 38 °C equal 66 hPa, i.e. the two climate conditions 20 °C/100% r.h. and 38 °C/100% r.h. differ in their absolute water partial pressure by a factor of 2.8. Accordingly, the acceleration factor between 20 °C/50% r.h. and 38 °C/90% r.h. is $2.8 \times 90/50 = 5$. Second, water diffusion through and solution of water in the barrier are temperature driven processes. Thus, even for constant absolute humidity, an increase in WVTR with temperature is expected – in first approximation this is an Arrhenius-like behavior using a material specific activation energy. However, such extrapolation of WVTRs can only be done if temperature and humidity have no other effects on the substrate and the barrier (e.g. loss of adhesion, thermo mechanical damage). Furthermore, the acceleration factor depends on the barrier material and therefore cannot simply be transferred from one barrier to another. Additionally, temperature changes can modify the barrier film permanently, e.g. by cracks due to different thermal expansion coefficients of organic and inorganic layers. Hence, calculating the WVTR for other conditions remains a critical step.

In this section we addressed issues related to transient durations and pre-conditioning as they have to be kept in mind for WVTR-measurements especially of multi-barrier stacks (see Fig. 1b).

3. Experimental

3.1. Permeation barrier film used for the study

A multi-layer barrier stack has been prepared on a polyethylene-terephthalate (PET) substrate as the barrier material for the evaluations carried out in this paper (the coated film PET including the multi-layer stack is subsequently referred to as "barrier film"). The main ideas behind multilayer stacks for high performance barrier layers have been described by several authors already and will not be discussed in this work (see e.g. Graff et al. [4] for details). The polymer substrate used in this study is Melinex® 400 CW PET film manufactured by DuPont Teijin Films which has been used as delivered without cleaning prior to barrier coating.

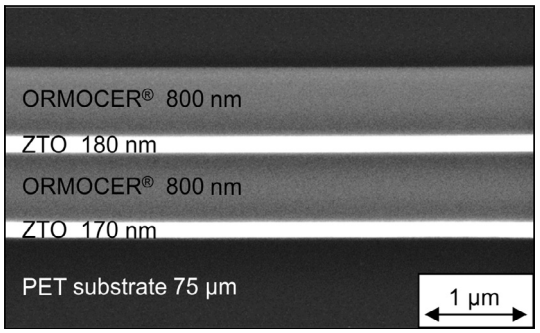

Fig. 2. SEM cross-section image of the multi-layer barrier structure used for the round-robin test in this paper.

The technology for manufacturing the layer stack is a joint development within the Fraunhofer Alliance POLO® in particular the institutes FEP, ISC and IVV and is described in detail elsewhere [6]. The layer stack used for this study consists of four layers as shown in Fig. 2.

The first and third layers on the substrate represent the oxide barrier material and are made of zinc-tin-oxide (Zn_2SnO_4 – ZTO) that has been applied by reactive dual magnetron sputtering. Thereby metal zinc-tin alloy targets with 52 wt.% zinc have been used. The reactive gas flow (oxygen) has been controlled using the optical emission of excited metal atoms in the plasma as the control variable in a proportional-integral–differential control loop.

The polymer interlayer is made of an ORMOCER® material. The term ORMOCER® describes organic–inorganic hybrid polymers with tailored properties for the specific application [7]. The layers have been applied to the substrate by using a reverse gravure printing process.

All layers have been coated in a roll-to-roll deposition process on a width of 220 mm in pilot scale machines described in an earlier paper [6]. The web speed was 0.5 m/min for the ZTO and 3 m/min for ORMOCER® coatings, respectively. One roll of this barrier film with a length of 50 m has been prepared for the evaluations in this study. The processing parameters and layer thicknesses have been kept constant over the 50 m coating length. Thereby a thickness deviation of less than ±5% for the ZTO barrier layers and of less than ±10% for the ORMOCER® interlayer has been measured using in-line optical transmission and reflection measurement. This is usually a range in which no significant change in the barrier performance of the layers is observed [8,9]. Reproducibility of the POLO® barrier film was investigated using a coulometric WVTR measurement device (BRUGGER WDDG). Samples taken from both the same roll used in this paper and rolls prepared under similar process conditions reproducibly yield a WVTR below the measurement limit of $1 \cdot 10^{-3}$ g/(m^2 d). An investigation on the reproducibility using a more sensitive method has not been conducted, yet. However in earlier studies, we found for a single sputtered ZTO layer, i.e. the first layer of the POLO® barrier film (see Fig. 2), a good reproducibility of the WVTR with a deviation of less than ±20% on the same substrate material and with an above-mentioned thickness deviation within one longer roll.

3.2. Sample preparation and test methods

3.2.1. Permeation measurement using a calcium-mirror-test

Pure metallic calcium is an opaque material and an electrical conductor. It reacts with water to form transparent and nonconductive calcium hydroxide, according to the following equation:

$$Ca + 2H_2O \rightarrow Ca(OH)_2 + H_2$$

If shielded by a barrier layer, the corrosion rate of a calcium thin-film is a measure of the water vapor transmission rate (WVTR) of the barrier: assuming an instantaneous consumption of all ingressing water by the residual calcium, the calcium corrosion rate can be directly translated into a WVTR of the encapsulation, i.e. the barrier., as it was described by Nisato et al. in 2001 [10].

The evaluation of the calcium tests relies on several assumptions, which are appropriate in the usual operation range. One of them is the selectivity to the reactive species, i.e. the question if calcium reacts only with water and there is no or negligible reaction of calcium with oxygen, as reported among others by Cros et al. and Reese et al. [11,12]. The fast reaction speed of the calcium and the assumption that all incoming water reacts with the calcium is reasonable, as calcium is a very ignoble material (redox potential of −2.87 V [13]). At last, a macroscopically homogenous corrosion of the calcium is assumed, which is not entirely correct for all cases, but does not impede with the validity of the results, if the test is designed properly, as it was examined by Klumbies et al. [14]. If the calcium thin-film is in close contact with the barrier to be characterized and not separated or averaged by a common gas volume, it has the ability to identify and measure local corrosion. This way, in an appropriate setup, the calcium test can distinguish between intrinsic and effective permeation and can identify the number, size and position of pinholes and defects, which often dominate the permeation through barrier films. Effective WVTR is the integral WVTR of a large area barrier, possibly including defects. Intrinsic WVTR is the ideal WVTR of the barrier material layer without (extrinsic) defects such as pinholes introduced by dust particles for example.

Another advantage of the calcium test is the option to quantify the calcium corrosion by optical or electrical measurements. Both options have specific advantages and drawbacks and exist in different variations.

In most configurations, the calcium test measures the total encapsulation performance of the thin-film, i.e. the combination of barriers on top, bottom and sides of the thin-film, as well as any interface permeation, as illustrated in Fig. 3. This cell might contain a cavity, filled with gas or an adhesive. Table 1 gives an overview over the calcium test methods used in this study.

3.2.2. Optical calcium test

The principle of the optical calcium test, developed at Philips Research is presented in [10]. The optical transmission of a thin calcium layer between barrier films is measured with a white spectrum (e.g. fluorescent EL lamp) light source and a CCD camera or a photodiode as the detector.

During oxidation of the calcium film, caused by the water vapor ingress through the barrier, the calcium corrosion rate (which is proportional to the WVTR) can be measured by two principles or a superposition of both. One option is to use a CCD camera to quantify the area of oxidized calcium and to determine the area growth rate or WVTR this way. The other option is to measure the averaged transmission of a larger area and assume a homogenous oxidation of the calcium thin-film. The resulting

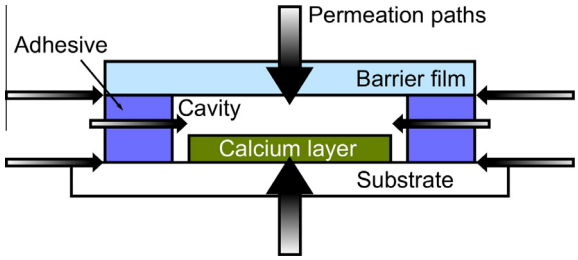

Fig. 3. schematic of a calcium test cell and illustration of residual permeation paths into the cell: The calcium thin film (“sensor”) is encapsulated by two barrier films on top and bottom plus an adhesive perimeter seal. The sensor measures the combined permeation rates of all these barriers plus additional water vapor ingress via interfacial permeation. The cavity is nitrogen filled.

change in optical transmission can be used to calculate a residual calcium thickness during ongoing measurement, for instance using Beer–Lambert’s law. At FhG-IAP, the optical attenuation coefficient α was calculated to $\alpha_{Ca} = 0.0478\ nm^{-1}$ using optical constants from Ramsdale and Greenham [15]. By using an optical detector such as a CCD, a combined method, calculating the local calcium thickness for each pixel with Beer–Lambert’s law, can be used and gives quantitative results (see for example Klumbies et al. [14].)

The optical calcium test was performed in four different laboratories within the presented inter-laboratory study: PHILIPS: Philips Research Laboratories and the Holst Centre; CSEM: Centre Suisse d’Electronique et. de Microtechnique SA, Muttenz Switzerland; CPI: Centre for Process Innovation, Redcar, UK; and FhG-IAP: Fraunhofer Institute for Polymer Research. To allow for better comparison of the methods, all optical calcium test samples used in this study were prepared at PHILIPS using the same sample design. Shipping was performed in inert atmosphere. At PHILIPS, 6 in. substrates of the barrier film are introduced from a glovebox (<1 ppm oxygen and water) to a vacuum chamber ($<10^{-6}$ mbar). In this chamber, calcium (40 nm) is directly deposited on the barrier side of the barrier film by thermal evaporation. In order to use statistics, the calcium pattern applied to each 6-in. substrate consists of 9 separate areas representing single samples on the same substrate. Each of these samples again consists of a cluster of 9 individual calcium pads of $5 \times 5\ mm^2$. Hence, there are 81 individual calcium pads per test substrate. This test substrate design is applied to limit the effect of (large) pinholes in the barrier. Especially, when a single inorganic barrier layer is being tested, the effect of pinholes can destroy a large-area single calcium pad on a relatively short time scale. The high water vapor transmission through pinholes causes local hydrolysis of the calcium layer, frequently followed by delamination of the layer and layer cracking. By dividing the calcium sample into 9 individual calcium pads, the reduction of calcium area by the presence of a large pinhole and a local barrier failure is limited to one pad. After calcium deposition and one night of storage in an inert gas glovebox, the whole barrier side of the barrier film, i.e. also the calcium, is coated with a high performance thin film barrier with well-known

Table 1
Calcium mirror test overview. Metrological characteristics of the single tests are presented. Ca-CCD: calcium test with a CCD camera, Ca-OD: calcium test with a photo-diode detector, Ca-E: electrical calcium test.

Technique	Laboratory	Metrological characteristics
Ca-CCD	PHILIPS	Intrinsic WVTR, Ca deposited on barrier, back encapsulated with PHILIPS barrier stack (w/o cavity), residual calcium determined optically for each single CCD-pixel using Beer–Lambert law
Ca-CCD	CSEM	Effective WVTR, Ca deposited on barrier, back encapsulated with PHILIPS barrier stack (w/o cavity), residual calcium determined optically for each single CCD-pixel using Beer–Lambert law
Ca-OD	CPI	Effective WVTR, Ca deposited on barrier, back encapsulated with PHILIPS barrier stack (w/o cavity), residual calcium determined optically using integral optical density and Beer–Lambert law
Ca-OD	FhG-IAP	Effective WVTR, Ca deposited on barrier, back encapsulated with PHILIPS barrier stack (w/o cavity), residual calcium determined optically using integral optical density and Beer–Lambert law
Ca-E	CEA-LITEN	Effective WVTR, Ca deposited on glass, barrier glued onto sensor (w/o cavity), residual calcium determined electrically monitoring calcium film conductance vs. time
Ca-E	TUD-IAPP	Effective WVTR, Ca deposited on barrier, back encapsulated using cavity glass (w/cavity), residual calcium determined electrically monitoring calcium film conductance vs. time
Ca-E	CSEM	Effective WVTR, Ca deposited on barrier, back encapsulated using cavity glass (w/cavity), residual calcium determined electrically monitoring calcium film conductance vs. time

characteristics representing the back encapsulation of the calcium. For better handling and mechanical stability, the barrier film is then placed on 6-in. glass plates using Kapton tape (polyimide) at the edges for fixing with the high performance thin film barrier facing towards the glass. The measured WVTR is the sum of the permeation through both barriers (barrier film under test and high performance thin film barrier). If one of the barriers is superior with respect to the other, the measured WVTR corresponds to the poorest barrier (highest WVTR). For this study, a three layer top barrier stack (developed by Philips/HOLST Centre) was used as top barrier with the layer structure silicon nitride/organic planarization coating/silicon nitride [16]. This top barrier shows a (effective) WVTR below 10^{-6} g/m^2 d at 38 °C/90% relative humidity (r.h). Therefore, any measured WVTR > 10^{-5} g/m^2 d can be attributed fully to the permeation through the barrier film.

The same samples measured at PHILIPS were provided to CSEM, FhG IAP and CPI for independent optical calcium test measurements.

Due to the use of a CCD-camera, a distinction can be made between the intrinsic permeation properties of the layer and the effective permeation properties. PHILIPS determined the intrinsic WVTR by excluding white areas on the calcium layer larger than $50 \times 50\ \mu m^2$. The time to measure was sufficient for at least 1 nm of calcium to be corroded. No transient regime was observed in this experiment. Note that the possibility of monitoring calcium corrosion in the sub-nm regime results from averaging the calcium height over a large number of pixels of the CCD-camera. At 1 nm reduction of a total Ca-height of 40 nm, we assume that we can measure the reduction of height with a precision of 5%. CSEM performed optical calcium tests in a very similar manner as described above. The only difference is that in CSEM measurement protocols, pinholes were taken into account in this study, i.e. CSEM measured an effective WVTR. Further details on the methods applied by can be found in [17].

The set-up of the optical calcium test at FhG-IAP followed the description from Hergert et al. [18]. The optical transmission is measured from a white LED used a light source and a photodiode for the detection of the light transmitted through the calcium layer. Typically, the measured spot had a diameter of about 3 mm resulting in the measurement of an effective WVTR including pinholes. Up to five samples are installed in a removable frame which was stored under different environmental conditions. The different samples and several measurement spots on a sample were selected by moving the frame with a stepping motor. CPI made transmission measurements of the calcium pad using a commercial optical densitometer (Barberi Densy 450e). This effectively shone a white light source through the sample with a photoelectric cell as a detector. The detection aperture was a 3 mm diameter measurement spot making this an effective WVTR measure i.e. transmission through pinholes was included.

3.2.3. Electrical calcium test

The electrical calcium test was performed in three different laboratories within the presented inter-laboratory study. In the following sections, the laboratories are referred to as: TUD-IAPP: Institut für Angewandte Photophysik at the Technical University of Dresden, Germany; CEA-LITEN, Grenoble, France; CSEM.

The electrical calcium corrosion test monitors the electrical resistance of a thin calcium layer (60–1000 nm thick) over time. The WVTR is calculated from the resistance change according to Paetzold et al. [19]. Laterally homogeneous calcium corrosion, i.e. a homogeneous height of residual calcium over the whole layer at any time, was assumed for the calculations in this study. This assumption of homogeneity obviously does not hold true for a calcium layer close to a barrier layer with defects (pinholes) that cause local corrosion. Surprisingly, it does not apply to a bare calcium layer, as corrosion starts at separated nuclei [20]. Still, in both cases the homogeneous-corrosion formula according to Paetzold et al. [19] yields nearly the correct corrosion rate and consequently can be used to extract the effective WVTR of the barrier [20,21]. Furthermore, the formula assumes a constant resistivity of the calcium, independent of its thickness. The resistivity of calcium is reported to range between $6.2 \cdot 10^{-8}$ Ω·m (measured at TUD-IAPP) and $8.95 \cdot 10^{-8}$ Ω m [19] for thermally evaporated thin-films of calcium. Note, that series

resistances, e.g. caused by the evaporated electrode, can dramatically distort the resistivity measurement [22]. More details about the method itself can be found in the literature [20].

At TUD-IAPP, the FhG-POLO® barrier film is degassed on a hot plate at 80 °C in a nitrogen-filled glovebox over 4 days before a 60 nm thick calcium rectangle of 4×17 mm^2 and aluminum electrodes were evaporated directly onto the barrier film. A cavity glass was glued onto the film via UV-curable glue (XNR 5590, Nagase Chemtex Corporation) to protect the back side of the calcium layer against ambient moisture (see [22] and [23] for details). The electrical resistance of the calcium layer was monitored during 1278 h of exposure of seven identical test cells to controlled conditions (38 °C/90% r.h., setup details in [24]). The WVTRs were calculated from the constant slope in the conductance-vs-time curves reached after approx. 400 h of measurement. Note that the WVTR of the POLO® barrier film is close to the background rate of the specific back-encapsulation used at TUD-IAPP at this time.

At CEA-LITEN, a 25 μm thick pressure sensitive adhesive was laminated onto the permeation barrier film and the stack was degassed at 80 °C under vacuum during 24 h before introduction into a glovebox. Calcium was evaporated on glass substrates with already deposited aluminum electrodes. The encapsulation system was then laminated (acrylate-based pressure sensitive adhesive from 3M) onto the calcium coated glass substrates on full area, i.e. without a nitrogen filled cavity. Finally the samples were stored for 1250 h for ageing in a climate chamber. The WVTRs were calculated from the constant slopes in the conductance-vs-time curves between 288 and 648 h of measurement.

CSEM followed a similar protocol for preconditioning, calcium evaporation and encapsulation in glovebox as TUD-IAPP. The size of the calcium pads evaporated on aluminum contacts was of 8×12 mm^2. The samples were encapsulated using a glass cavity and UV-cured edge seal (protocol as in [22]). The samples were stored in cleanroom controlled conditions for the ambient condition and in environmental chambers for the tropical condition. The WVTRs were calculated from the constant slopes in the conductance-vs-time curves with measurement times ranging from 220 h (tropical conditions) to 700 h (ambient conditions).

3.2.4. Cavity ringdown spectroscopy (CRDS)

CRDS measurements have been performed at the National Physical Laboratory, United Kingdom (thereafter referred to as NPL). The CRDS analyzer detects water vapor by tuning a laser source to an absorption line of water and is described in [25]. The system is designed to be symmetrical around a single "dry" chamber separated from two "wet" chambers by two samples of the barrier material under test with the barrier layers facing the "dry" side. Two 10×10 cm^2 samples of barrier material are attached to a central stainless steel support with a thin layer of ultra-high vacuum grease (Fomblin®, Solvay Specialty Polymers; approximately 1 cm from the perimeter). The barrier layers are sandwiched between two stainless steel outer discs and a central support. The whole assembly is held firmly in place with a G-clamp. No pre-conditioning was employed for the samples used in the present work.

3.2.5. Tunable diode laser absorption spectroscopy (TDLAS)

TDLAS was used at the Fraunhofer Institute for Materials and Beam Technology (FhG-IWS, Dresden, Germany). This method enables the detection of water vapor transmission rates down to 10^{-5} g/m^2 d and below. The TDLAS based instrument uses the common isostatic setup with a dry nitrogen carrier gas flow (carrier gas mode). Therefore a standard permeation cell consisting of a feed and a permeate compartment separated by the barrier sample has been used. To prevent leakages and unwanted permeation through the sample edges, the common sealing concept (O-ring) has been substituted by dry nitrogen purged sealing channels. The detection principle is based on the measuring of the attenuation of the laser light intensity caused by the excitation of the permeated water molecules. Further details on the TDLAS setup and the measurement modes can be found in Beese et al. [26]. In the measurement setup the temperature within the permeate and feed compartment was kept at 38 °C and 20 °C, respectively, for the tests in this study. The humidity at the feed side is generated by a two-pressure water vapor generator that is placed directly above the feed compartment. This water vapor generator provides a relative humidity between 50% and 95%. A 100% relative humidity is provided by a water soaked glass frit.

3.2.6. Isotope marking mass spectrometry (IMMS)

IMMS was performed at the Institut National De L'Energie Solaire INES, Chambéry, France (CEA-INES). The method is described in [27,28]. The permeation measurement cell comprises two test chambers separated by the test-sample which is a disc with a diameter of 65 mm. The first gas chamber is filled with the test gas. A constant concentration in target gas is maintained in the upstream side (first chamber) and a concentration close to zero is maintained in the downstream side (second chamber) using continuously a high vacuum pumping system (vacuum level in the range of 10^{-8} mbar). Gas molecules that permeated through the test sample are detected using a mass spectrometer. The use of mass spectrometry makes it possible to measure several types of gases including water and oxygen. In this study, deuterated water (D_2O) was used as test gas. The samples were preconditioned at 38° under vacuum for 1 month. During the measurements, the samples are mechanically supported by a porous material and clamped with a double O-ring system.

3.2.7. Coulometric test

Coulometric measurements were carried out using a commercial Mocon Aquatran® device and were performed in two different laboratories: FhG-IVV (Fraunhofer Institute for Process Engineering and Packaging IVV) and CPI (Centre for Process Innovation). At the beginning of this study, the MOCON Aquatran® Model 1 water vapor permeation measurement system was the only commercially available system that is able to measure a WVTR down to $5 \cdot 10^{-4}$ g/(m^2 d). In the device, the measurement cell is divided by the sample into two chambers. In one chamber,

a constant relative humidity and temperature is maintained. The second chamber is purged using a carrier gas (dry nitrogen) which guides the permeated water molecules to a coulometric sensor. The sensor itself is based on phosphorous pentoxide (P_2O_5) coated electrodes. The P_2O_5 absorbs all incoming water molecules which are then electrolyzed by a voltage across the electrodes. Therewith an electrical current between the electrodes is induced that is measured and used to calculate the WVTR [29]. In this study, the measurements were performed at 38 °C/90% r.h. and 20 °C/50% r.h., respectively. In all cases, the coated side of the barrier film was facing toward the nitrogen gas purged low humidity measurement chamber. The samples have been taken directly from the laboratory atmosphere for measurement without any prior drying/preconditioning.

4. Results and discussion

The permeation rates reported by the different groups are given in columns 2 and 5 of Table 2 for the two chosen nominal measurement conditions, namely 20 °C at 50% (r.h.) and 38 °C at 90% r.h. Thereby the uncertainty for the storage temperature was (20 ± 1) °C and (38 ± 1) °C, and the uncertainty for the relative humidity was (50 ± 5)% and (90 ± 3)% or better.

Each measurement was performed typically in duplicate and in several cases with as many as 9 samples per condition (see Experimental section), the number is given by n. The experimentally derived standard deviations, σ, are reported in column 3 and 6.

The acceleration factor F (given in column 8) represents the ratio between the permeation rates at the two nominal conditions - ambient and tropical. In addition to the barrier behavior of the barrier substrates (“activation energy of permeation”), this factor is a combination of a factor of 1.8 for the change in relative humidity between the two measuring conditions and 2.83 for the temperature dependence of the absolute humidity at the two measurement temperatures. All calcium tests measured a significantly lower acceleration factor than 5.1 (=1.8 · 2.83); TDLAS, however, measured F = 6.76. For these calcium tests as well as for TDLAS, the measured WVTRs were well within the detectable range. Hence, reaching the limit of detection and, thus, obtaining an erroneous factor between the two climate conditions cannot explain the present deviations in the measured acceleration factors. A detailed discussion on an appropriate model to estimate the acceleration factor as well as an explanation for the observed deviations are outside the scope of this paper and have to be part of future research. We would simply like to stress that the temperature dependence of permeation through the sample is a property of the barrier film and may well vary between different types of high performance barrier systems. Therefore one cannot simply assume that the acceleration factor between different measurement conditions for one given barrier film will necessarily apply to another barrier film. Again, please note that in this study only one barrier type was used.

The geometries and dimensions of the sample tested vary due to the requirements and constraints of the measurement principles. Since this can be a reason for variability, the typical sample dimensions are listed separately. The total measured area refers to the actual sample area taken into consideration for the permeation measurement. In order to reflect real-life conditions, usually the larger the better. On the other hand this can lead to problems when only small samples are available at early research stages. Also, large samples are more prone to external damage sources during measurement such as large scratches which potentially result in a too high WVTR that does not represent the property of the film itself. For most techniques the “spot size” also corresponds to the total measured area. For optical calcium tests (and especially for imaging based calcium tests), the total area measured can be increased by combining the data from several spots.

Table 2
Summary of experimental results. Ca-CCD: calcium test with a CCD camera Ca-OD: calcium test with a photo-diode detector, Ca-E: electrical calcium test, CRDS: Cavity Ring Down Spectroscopy, TDLAS: Tunable Diode Laser Absorption Spectroscopy; IMMS: Isotope Marking Mass Spectrometry. Coulometric: Mocon Aquatran Model 1. The lower sensitivity limit, in ambient conditions, is either the limit of detection according to the manufacturer (for coulometric devices) or the WVTR measured for an absolute barrier like glass or stainless steel, e.g. caused by the non-perfect back encapsulation (for all other methods).

Technique	Ambient (20 °C/50% r.h.) (g/(m² d))			Tropical (38 °C/90% r.h.) (g/(m² d))			F	A_{spot} (cm²)	A_{meas} (cm²)	Effective	Lower limit of sensitivity (g/(m² d))	Laboratory
	WVTR	σ	n	*WVTR*	σ	n						
Ca-CCD-1	$7.86 \cdot 10^{-5}$	$1.23 \cdot 10^{-5}$	18	$2.78 \cdot 10^{-4}$	$5.4 \cdot 10^{-5}$	17	3.54	0.063	0.563	No	$<10^{-6}$	PHILIPS
Ca-CCD-2	$1.56 \cdot 10^{-4}$	$1.7 \cdot 10^{-5}$	9	$5.33 \cdot 10^{-4}$	$4.2 \cdot 10^{-5}$	9	3.42	0.04	0.36	Yes	$<10^{-6}$	CSEM
Ca-OD-1	$4.90 \cdot 10^{-5}$	$1.2 \cdot 10^{-5}$	9	$1.20 \cdot 10^{-4}$	$4.0 \cdot 10^{-5}$	8	2.45	0.071	0.563	Yes	$1.2 \cdot 10^{-5}$	CPI
Ca-OD-2	$7.00 \cdot 10^{-5}$	$1.5 \cdot 10^{-5}$	9	$1.60 \cdot 10^{-4}$	$2.0 \cdot 10^{-5}$	3	2.29	0.07	1.89	Yes	$<1 \cdot 10^{-5}$	FhG-IAP
Ca-E-1	n.a.	n.a.	n.a.	$6.60 \cdot 10^{-4}$	$3.3 \cdot 10^{-4}$	2	n.a.	0.1	0.1	Yes	$2 \cdot 10^{-5}$	CEA-LITEN
Ca-E-2	n.a.	n.a.	n.a.	$5.37 \cdot 10^{-4}$	$1.31 \cdot 10^{-4}$	7	n.a.	0.64	0.64	Yes	$1 \cdot 10^{-4}$	TUD-IAPP
Ca-E-3	$1.70 \cdot 10^{-4}$	$1.5 \cdot 10^{-5}$	3	$6.40 \cdot 10^{-4}$	$1.0 \cdot 10^{-4}$	3	3.76	1.20	1.20	Yes	$1 \cdot 10^{-5}$	CSEM
CRDS	$1.40 \cdot 10^{-4}$	$3.9 \cdot 10^{-5}$	3	n.a.	n.a.	3	n.a	75.7	75.7	Yes	$3 \cdot 10^{-5}$	NPL
TDLAS	$4.23 \cdot 10^{-5}$	$2.5 \cdot 10^{-5}$	2	$2.86 \cdot 10^{-4}$	$6.3 \cdot 10^{-5}$	12	6.76	134	134	Yes	$1 \cdot 10^{-6}$	FhG-IWS
IMMS	n.a.	n.a.	n.a.	$1.30 \cdot 10^{-4}$	n.a.	1	n.a.	12	12	Yes	$5 \cdot 10^{-5}$	CEA-INES
Coulometric-1	$<5 \cdot 10^{-4}$	$5 \cdot 10^{-4}$	2	$6.5 \cdot 10^{-4}$	$5.0 \cdot 10^{-4}$	2	>1.3	50	50	Yes	$5 \cdot 10^{-4}$	CPI
Coulometric-2	n.a.	n.a.	n.a.	$7.0 \cdot 10^{-4}$	$2.8 \cdot 10^{-4}$	4	n.a.	50	50	Yes	$5 \cdot 10^{-4}$	FhG-IVV

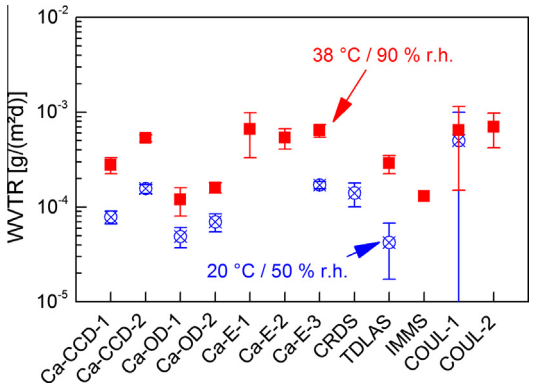

Fig. 4. Graphical representation of the WVTR result from the different laboratories. See Table 2 for details. The error bars are $\pm\sigma$.

In Table 2, A_{spot} (column 9) describes the size of a single measurement spot and A_{meas} (column 10) the total measurement area. For example, in optical imaging calcium test, one can exclude the edges of the sample or select specific areas that are pinhole free to measure intrinsic WVTR. In samples with large number of pinholes this can lead to significant differences between the intrinsic and the effective WVTR. This distinction is given in column 11. The last column (12) presents the laboratory that carried out the measurements. Some laboratories were unable, for practical, logistic or detection limit reasons, to provide data for both ambient and tropical conditions.

The permeation data are represented in Fig. 4, with error bars representing one standard deviation of the measurements. The figures illustrate that the different methods are in general agreement, with most results lying within one standard deviation.

Since variations in the order of 20–50% are usual for the same nominal samples at constant conditions, i.e. same method, operator, and laboratory, we found as our main result a satisfactory agreement in permeation measurement between the different methods. That there was no significant difference between intrinsic (Ca-CCD by PHILIPS) and effective WVTR (all other laboratories) in the barrier samples is either due to water vapor transmission occurring through a multitude of small defects in the barrier being not identified as single defects or due to the use of a multilayer barrier (see Section 2). While the general agreement between the different methods is satisfactory and actually better than initially expected by the authors, there are still significant differences and outliers.

The largest variations were noted on the commercially available coulometric system, having a detection limit of $5 \cdot 10^{-4}$ g/(m^2 d), which is unfortunately very close to the WVTR of the samples considered. FhG IVV measured additionally a high WVTR of $3.3 \cdot 10^{-3}$ g/(m^2 d), which is an outlier and probably caused by pinholes or cracks formed during the handling of these test specimens. However, since such cracks in the barrier are not visible, all samples were measured and included. This illustrates the practical difficulties that many laboratories would encounter testing good barriers with commonly available equipment.

While the influence of design details is expected to explain most of the residual scatter, explaining the residual scatter in detail is beyond the scope of this work and the subject of a further investigation.

In summary, our results clearly show that – besides outliers probably caused by design details of the single set-ups and handling – a satisfactory agreement on the WVTR in the same barrier film measured with different methods can be found.

So far a standard procedure for the WVTR evaluation of high performance barrier layers is missing. However, from our investigations we derive some aspects to clarify when writing reports on WVTRs: (i) Storing/pre-conditioning/initial state of the sample prior to the measurement. (ii) Does the experiment aim for the steady-state permeation, i.e. the WVTR, or the amount of water vapor accumulated over a given period of time. (iii) Measurement time and, when applicable, what was the criterion for determining that steady-state was reached? (iv) What are the climate conditions the measurement was carried out at? (v) For optical calcium tests: Were (point) defects eliminated from the analysis (intrinsic WVTR) and, if applicable, what is the detection threshold size applied? (vi) Was the sample measured in an accumulation mode (changing humidity on sensor side over time) or with constant boundary conditions. The proposal for a detailed standard procedure and conditions is beyond the scope of this paper.

5. Conclusions

The starting point of this work was the observation, reported in [1], that it is difficult to compare results between laboratories working with state of the art barriers and permeation methods, either obtained on the same materials or using similar methods. The tests actually comprise a number of different measurement techniques as well as test cell geometries, evaluated in different environmental conditions in different laboratories and on different barrier materials. This creates quite naturally some misunderstandings and inconsistencies. Moreover, opinions differ about the quantitative or qualitative nature of some of the methods. As a consequence there appears to be a remarkable amount of unnecessary duplication of work in the community in the absence of clear guidelines, standardized testing conditions and equipment.

We have shown in the work that the so called calcium tests performed in different laboratories shows a remarkable quantitative agreement with one another and with a range of state of the art permeation methods, including TDLAS, CRDS, IMMS and Coulometric Measurement. Reducing the testing conditions to two well defined sets was a trivial but important step for an effective comparison. The results are encouraging to further investigate and propose characterization methods to relate lifetime of devices to barrier properties, related to intrinsic degradation modes of printable and organic electronic devices for example. We observed also variations between methods which may be reduced by applying a common set of recommendation and guidelines, especially to perform optical and electrical calcium tests. These are the subject of ongoing work and future publications.

Acknowledgements

We would like to acknowledge Marion Schmidt (formerly Fraunhofer IVV), Oliver Miesbauer (Fraunhofer IVV), Sabine Amberg-Schwab and Ulrike Weber for their support on preparing the barrier film samples and the Aquatran measurements at Fraunhofer IVV. We thank Olaf Zywitzki and Thomas Modes (Fraunhofer FEP) for providing the SEM cross section images of the barrier film. We are grateful to Guillaume Basset and Marek Chrapa for their contributions to the calcium test measurements at CSEM. We thank Harald Beese (Fraunhofer IWS) for the the TDLAS measurements. We are grateful for the support of the Printable and Organic Electronic association (OE-A) in providing a working group platform on encapsulation that made this collaboration possible. We gratefully acknowledge financial support of national and international public bodies including: The German Federal Ministry for Education and Research BMBF (Ref. No. 13N8858, 13N11059, and 03IPT602A) and the European Commission (project OLATRONICS) for support on the development of the barrier film used in this study, the UK BIS National Measurement System's Chemistry Biology measurement program. The round robin calcium test was facilitated by the financial support of the Holst Centre in processing of the calcium samples.

References

[1] G. Nisato, Encapsulation survey report, Deliverable WP5 OPERA FP7 project <http://www.csem.ch/docs/Show.aspx/27588/docname/OPERA-encapsulation-survey-2010.pdf>.
[2] A.P. Roberts, B.M. Henry, A.P. Sutton, C.R.M. Grovenor, G.A.D. Briggs, T. Miyamoto, M. Kano, Y. Tsukahara, M. Yanaka, J. Membr. Sci. 208 (2002) 75.
[3] N. Kim, W.J. Potscavage Jr., A. Sundaramoothi, C. Henderson, B. Kippelen, S. Graham, Sol. Energ. Mat. Sol. Cells 101 (2012) 140.
[4] G.L. Graff, R.E. Williford, P.E. Burrows, J. Appl. Phys. 96 (2004) 1840.
[5] O. Alduchov, R. Eskridge, J. Appl. Meteorol. 35 (1996) 601.
[6] J. Fahlteich, S. Amberg-Schwab, U. Weber, K. Noller, O. Miesbauer, C. Boeffel, N. Schiller, SID 2013 Digest (2013) 354.
[7] K.-H. Haas, Adv. Eng. Mater. 2 (9) (2000) 571.
[8] J. Fahlteich, M. Fahland, W. Schönberger, N. Schiller, Thin Solid Films 517 (10) (2009) 3075.
[9] J. Fahlteich, W. Schönberger, M. Fahland, N. Schiller, Surf. Coat. Technol. 205 (2) (2011) S141.
[10] G. Nisato, P.C.B. Bouten, P.J. Slikkerveer, W.D. Bennett, G.L. Graff, N. Rutherford, L. Wiese, in: Proc. 21st Annual Asia Display, 8th Intl. Display Workshop, 2001, p. 1435.
[11] S. Cros, M. Firon, S. Lenfant, P. Trouslard, L. Beck, Nucl. Instrum. Methods Phys. Res. B: Beam Interact Mater. Atoms 251 (2006) 257.
[12] M.O. Reese, A.A. Dameron, M.D. Kempe, Rev. Sci. Instrum. 82 (2011) 085101.
[13] D.R. Lide, Handbook of Chemistry and Physics, 73rd ed., CRC Press Inc., Boca Raton, 1992.
[14] H. Klumbies, L. Müller-Meskamp, T. Mönch, S. Schubert, K. Leo, Rev. Sci. Instrum. 84 (2) (2013) 024103.
[15] C.M. Ramsdale, N.C. Greenham, J. Phys. D: Appl. Phys. 36 (2003) L29.
[16] A. van Mol, P. van de Weijer, C. Tanase, Proc. SPIE 6999–46 (2008).
[17] P.C.B. Bouten, G. Nisato, P.J. Slikkerveer, H.F.J.J. van Tongeren, E.I. Haskal, P. van der Sluis, US Patent No. 6993956, 2006.
[18] S. Hergert, M. Linkor, M. Korny, N. Fruehauf, J. Soc. Inf. Display 15 (6) (2007) 421.
[19] R. Paetzold, A. Winnacker, D. Heseler, V. Cesari, K. Heuser, Rev. Sci. Instrum. 74 (2003) 5147.
[20] H. Klumbies, L. Müller-Meskamp, T. Mönch, S. Schubert, K. Leo, Rev. Sci. Instrum. 84 (2013) 024103.
[21] R. Paetzold, D. Henseler, K. Heuser, V. Cesari, W. Sarfert, G. Wittmann, A. Winnacker, Proc. SPIE 5214 (2004) 73.
[22] S. Schubert, H. Klumbies, L. Müller-Meskamp, K. Leo, Rev. Sci. Instrum. 82 (2011) 094101.
[23] H. Klumbies, L. Müller-Meskamp, F. Nehm, K. Leo, Rev. Sci. Instrum. 85 (2014) 016104.
[24] H. Klumbies, L. Mueller-Meskamp, S. Schubert, T. Moench, M. Hermenau, K. Leo, in: 56th Annual Technical Conference Proceedings of the Society of Vacuum Coaters, 2013, pp. 362–368.
[25] P.J. Brewer, B.A. Goody, Y. Kumar, M.J.T. Milton, Rev. Sci. Instrum. 83 (2012) 075118.
[26] H. Beese, W. Grählert, S. Kaskel, J. Grübler, J. Koch, K. Pietsch, in: Proceedings of the 2012 Web Coating & Handling Conference of the Association of Industrial Metallizers, Coaters and Laminators AIMCAL, 2012, p. 848, ISBN 978-1-622-76950-6.
[27] M. Firon, S. Cros, P. Trouslard, Method and device for measurement of permeation, US Patent 7,624,621, 2009.
[28] A. Morlier, S. Cros, J.P. Garandet, N. Alberola, Thin Solid Films 550 (2014) 85–89.
[29] Mocon Inc., Aquatran® Model 1 Operator's Manual – Revision D, 2014. <http://www.mocon.com/distributor/pdfmanuals/Aquatran%20-%20d.pdf>.